1   *FT/FD-GRF5* repression loop directs growth to increase soybean yield

2   Kun Xu[1*], Xiao-Mei Zhang[1*], Guolong Yu[2*], Mingyang Lu[1*], Chunyan Liu[2*], Haifeng Chen[3*],

3   Jinlong Zhu[1], Fulu Chen[1], Zhiyuan Cheng[1], Penghui Huang[1], Xinan Zhou[3], Qingshan Chen[2],

4   Xianzhong Feng[4], Yuchen Miao[5], Liangyu Liu[6], Iain Searle[7], Yong-Fu Fu[1§]

5

6   [1] MOA Key Laboratory of Soybean Biology (Beijing), National Key Facility of Crop Gene

7   Resource and Genetic Improvement, Institute of Crop Sciences, Chinese Academy of

8   Agricultural Sciences, Nandajie 12, Zhongguancun, Haidian District, 100081 Beijing, China

9   [2] Key Laboratory of Soybean Biology, Ministry of Education/College of Agriculture, Northeast

10   Agricultural University, Harbin 150030, China

11   [3] Oil Crops Research Institute, Chinese Academy of Agricultural Sciences, Key Laboratory of

12   Biology and Genetic Improvement of Oil Crops, Ministry of Agriculture, Wuhan, 430062,

13   China

14   [4] CAS Key Laboratory of Soybean Molecular Design Breeding, Northeast Institute of

15   Geography and Agroecology, Chinese Academy of Sciences, Changchun 130102, China

16   [5] Key Laboratory of Plant Stress Biology, State Key Laboratory of Cotton Biology, School of

17   Life Sciences, Henan University, Kaifeng 475004, China

18   [6] College of Life Sciences, Capital Normal University, Beijing 100048, China

19   [7] School of Biological Sciences, School of Agriculture, Food and Wine, The University of

20   Adelaide, Adelaide, 5005, Australia.

21

22

23   [*] These authors contributed equally.

24

25   [§]To whom correspondence should be addressed. E-mail: fuyongfu@caas.cn or

26   fufu19cn@163.com. Telephone/Fax: +86-10-82105864

27

Abstract

Major advances in crop yield are eternally needed to cope with population growth. To balance vegetative and reproductive growth plays an important role in agricultural yield. To extend vegetative phase can increase crop yield, however, this strategy risks loss of yield in the field as crops may not mature in time before winter come. Here, we identified a repression feedback loop between *GmFTL/GmFDL* and *GmGRF5-1* (*Glycine-max-Flowering-Locus-T/Glycine-max-FDL* and *Glycine-max-GROWTH-REGULATING-FACTOR5-1*), which functions as a pivotal regulator in balancing vegetative and reproductive phases in soybean. *GmFTL/GmFDL* and *GmGRF5-1* directly repress gene expression each other. Additionally, *GmGRF5-1* enhances vegetative growth by directly enhancing expression of photosynthesis- and auxin synthesis-related genes. To modulate the loop, such as fine-tuning *GmFTL* expression to trade-off vegetative and reproductive growth, increases substantially soybean yield in the field. Our findings not only uncover the mechanism balancing vegetative and reproductive growth, but open a new window to improve crop yield.

Introduction

The global crop demand for human consumption and livestock feed is forecasted to increase by 110% from 2005 to 2050[1], while recent advances on traditional breeding, genomics and transgenic technology are predicted to only yield improvements of up to 20%[2]. Flowering time is widely used as a selectable marker in plant high-yield breeding programs[3], because vegetative growth is closely related to reproductive growth. A long vegetative phase means later flowering, larger and more vegetative organs (such as leaves and roots), that results in high yield because it provides the plenty source for yield formation. However, crops in the field may not mature normally before winter and lose the yield if the vegetative phase is too long[4]. Balancing vegetative and reproductive growth will achieve high yield in a normal growth season.

56   The transition from the vegetative to reproductive phase is regulated by a complex genetic

57   network that monitors and integrates both the plant developmental and environmental signals,

58   resulting in production of florigen *Flowering Locus T* (*FT*)[5,6]. The lower the florigen production,

59   the later the flowering and the higher the yield, and *vice versa*[3]. The *FT* dosage plays a key

60   role in the yield of tomato[7] and rice[8]. Not only function on flowering control, *FT* homologs also

61   contribute to the regulation of vegetative growth, such as tuberisation[9], onion bulb formation[10]

62   and sugar beet growth[11]. *FT* coordinates reproductive and vegetative growth in perennial

63   poplar[12]. Recently, *FT* was reported to regulate seed dormancy through *Flowering Locus C*[13].

64   *FT*, together with *FD* negatively correlates with leaf size as its overexpression leads to smaller

65   leaves and reduced expression leads to increased leaf size[6,14]. But, the mechanism of *FT* in

66   regulating the development and function of leaves is still uncovered.

67

68   *GROWTH-REGULATING-FACTOR* (*GRF*) family genes encode plant-specific transcriptional

69   factors, which are shown to bind DNA with a TGTCAGG *cis*-element to repress or activate the

70   expression of their target genes[15,16]. *GRF5* is confirmed as a key regulator of leaf growth and

71   photosynthetic efficiency by enhancing cell division and chloroplast division, with concomitant

72   increases in leaf size, longevity and photosynthesis[17]. Additonally, *GRF5* and cytokinins

73   synergistically function in leaves[17]. Also, there are no direct target genes of *GRF5* in leaves

74   identified yet.

75

76   Based on these observations, we hypothesised that *FT* participated in leaf development and

77   then it is possible to gate *FT* expression to an extent that ensures that soybean to flower

78   slightly later yet matures in the field before the low winter temperatures arrive, thereby

79   increasing yield. In this study, we demonstrated that in soybean *GmFTL/GmFDL* directly

80   inhibited *GmGRF5-1* expression; in turn, *GmGRF5-1* directly repressed *GmFTL* expression.

81   Therefore, we established a repression feedback loop, which balanced vegetative growth and

82   reproductive growth. Fine-tuning this loop by controlling *GmFTL* expression delayed flowering

83   and increased yield in the field. *GmGRF5-1* directly activated genes related to energy

84   metabolism (photosynthesis) and organ growth, which could all contribute to yield formation in

85   soybean. Our results indicated that the *GmFTL/GmFDL-GmGRF5* repression loop was a new

86   target to improve crop yield.

87

88   **Results**

89   **Gating *GmFTL* expression increases yield**

90   To test whether *GmFTL* controls soybean yield, we employed four selected transgenic lines of

91   *GmFTL*-RNAi, which had lower expression of *Glycine max FT-like*s (*GmFTL*s) and later

92   flowering[18]. Unsurprisingly, the soybean transgenic lines obviously showed high yield in both

93   a growth chamber and greenhouse, and *GmFTL*-RNAi line 4 doubled yield per plant in the

94   greenhouse (Fig. 1a, b). To obtain practical data in the field, we grew these soybean plants in

95   two regions (Hanchuan and Beijing: N30°22', E113°22' and N39°58', E116°20', respectively).

96   As a result of later flowering, only two lines (#1 and #3) matured normally in the growth

97   season. These two lines significantly displayed higher yield, ranging from 14% to 62%,

98   depending on the transgenic lines, locations and sowing time (Fig. 1c). TaqMan PCR data

99   indicated that high yield related to lower expression of *GmFTL3*, a major florigen in

100   soybean[19,20] and that the level of *GmFTL3* transcripts was inversely proportional to yield (Fig.

101   1d). Together, florigen negatively contributed to plant yield.

102
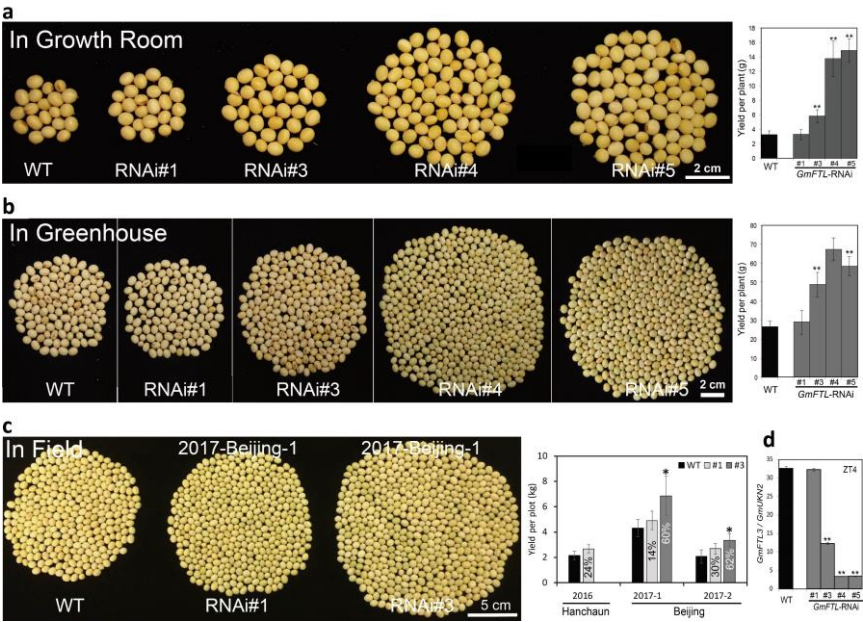
103   **Fig. 1 Reducing *GmFTL* expression increases soybean yield. a**, **b** and **c**,

104   Soybean yield in the growth room (**a**), glasshouse (**b**) and field (**c**). Left panels show

105   the total number of seeds per plant. Right panels show the quantified yield per plant

106   or plot. The percentages shown in the columns (**c**) indicate the increased yield

107   compared to wild type. **d**, The mRNA abundance of *GmFTL3* in different transgenic

108   lines. (* *P* < 0.05 and ** *P* < 0.01 , Student's *t*-test, n ≥ 10 plants).

109

110   **Yield increase contributed by photosynthesis**

111 We next performed experiments to explain how *GmFTL* controlled soybean yield through

112 growing *GmFTL*-RNAi lines in the greenhouse to analyse vegetative growth in detail. In the

113 early stage of growth, there was little difference in the architecture between the transgenic

114 and wild type plants. Along with growth, all RNAi lines displayed larger stature, with higher

115 plants, more nodes, larger leaves and roots compared to WT, companying with later flowering

116 and podding and high yield (Extended Data Fig.1, 2). Our results were consistent with a

117 previous report on genome-wide association analysis for flowering and yield, which indicated

118 a close correlation between plant height, flowering time and yield in soybean[21].

119

120 Photosynthesis efficiency significantly affects plant yield[22]; thus, we wondered whether there

121 was a change in the photosynthesis of the transgenic lines compared to the wild type plants.

122 Transmission electron microscope revealed that the transgenic lines had a much more

123 complicated structure in the chloroplast, with more and wider thylakoid membranes and rich

124 grana in both the vegetative stage (the third trifoliolate opening) and flowering stage (the

125 seventh trifoliolate opening) (Fig. 2a, Extended Data Fig. 3a). The detailed phenotypes are

126 following (Fig. 2b, c, Extended Data Fig. 3b, c). Compared to wild type plants, the total

127 number of chloroplasts (TNC) per cell of RNAi lines was lower, yet TNC per leaf area was

128 higher in the vegetative stage because of the smaller cell size (CS). After flowering, the

129 transgenic lines had larger CS and a lower TNC per leaf area. However, due to more and

130   larger leaves, the transgenic lines had more TNC per plant at this stage. Transgenic cells also

131   enriched different photosynthetic pigments (Fig. 2d).

132

133   Therefore, it was unsurprising that a biochemical assay evidenced that *GmFTL*-RNAi lines

134   had much higher yield of the maximum quantum and photosynthetic rates (Figure 2d) and

135   accumulated much more photosynthetic assimilates, such as starch, sucrose, glucose and

136   fructose (Figure 2e). Thus, the transgenic *GmFTL*-RNAi plants had higher photosynthesis

137   efficiency than did the wild type plants. Thus, the transgenic *GmFTL*-RNAi plants had higher

138   photosynthesis efficiency than did wild type plants, which conferred to high yield as previous

139   studies reported[22].

140
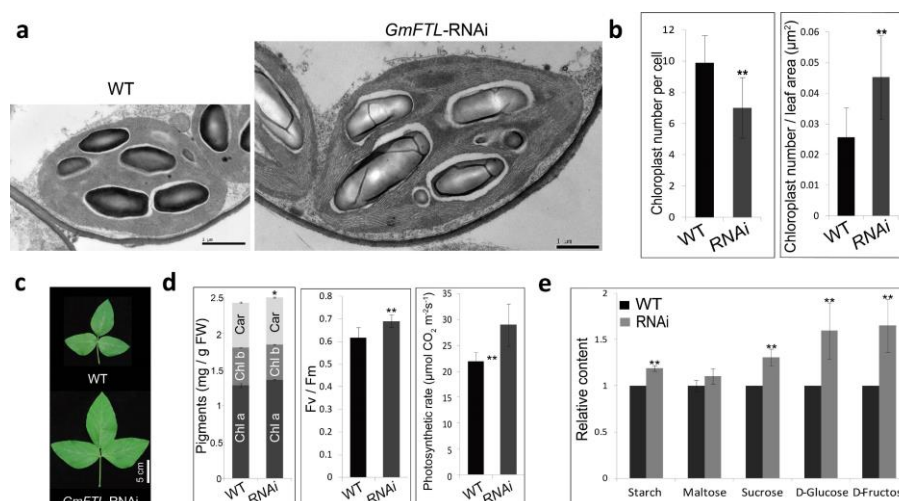
141   **Fig. 2 Reducing *GmFTL* expression enhances soybean leaf photosynthesis**. **a**,

142   The chloroplasts in the third trifoliolates. Scale bar, 1 μm. **b**, The average number of

143   chloroplasts per cell and per leaf area in the third trifoliolates (n= 30 plants). **c**, The

144   seventh trifoliolates. **d**, The amounts of chlorophyll a, b and carotenoids, the

145   maximum quantum yield and the net photosynthesis (n= 5-10 plants). **e**, The

146   contents of sugars in the 3rd trifoliolates (n= 10 plants). Statistical analysis was done

147   as Fig. 1.

148

149   *GmFTL3/GmFDL* **directly inhibits *GmGRF5-1* gene**

150   During the floral transition, FT enhances flowering by interacting with FD in the shoot

151   meristem, and FD binds to G-Box on its target genes[23]. *Arabidopsis GRF5* encodes a plant-

152   specific transcription factor and regulates many plant-specific processes, such as chloroplast

153   growth, photosynthesis and leaf growth[17]. The closest homolog of *GRF5* in soybean,

154   *GmGRF5-1* (*Glycine max GRF5-1*), coded the protein shared highly conserved functional

155   domains and localised in the nucleus (Extended Data Fig. 4a, b) as a transcriptional factor

156   did. And in the promoter sequence of *GmGRF5-1*, there are two typical G-Box motifs, the

157   binding site of bZIP transcription factor (such as FD) (Extended Data Fig. 5a). Together, we

158   wondered if GmFDL may target directly *GmGRF5-1*, that in turn regulated photosynthesis.

159

160   Then we performed electrophoretic mobility shift assays (EMSA), and the results

161   demonstrated that GmFDL5 (*Glycine max* FD-like5) proteins physically interact with G-Box I

162   (Fig. 3a). Transcriptional activity analysis of transient expression in tobacco leaves indicated

163   that *GmFDL5* inhibited *GmGRF5-1* promoter activity, and *GmFTL3*, the most likely candidate

164   of florigen in soybean[19,20], enhanced the effect of *GmFDL5* (Fig. 3b). Another FDL homolog,

165   GmFDL1, also displayed inhibitory activity on the *GmGRF5-1* promoter (Fig. 3c). GmFTL3

166   proteins interacted with both GmFDL5 and GmFDL1 (Fig. 3d, Extended Data Fig. 6), that is

167   consistent with a previous report[24]. To confirm the binding activity of *GmFDL in vivo*, we

168   performed ChIP-qPCR with hair roots expressing *GmFDL5:GFP* and leaves of

169   overexpressing *GmFDL1:GFP* plants, which showed early flowering (Fig. 3h). Both

170   experiments identified that *GmFDL5*/*GmFDL1* enriched Fragment 4 of *GmGRF5-1* promoter

171   (Fig. 3e). Further, the TaqMan PCR test exhibited that reducing *GmFTL* expression increased

172   *GmGRF5-1* expression but had little effect on *GmFDL* expression (Fig. 3f). Therefore, we

173   postulated that GmFDL functioned mainly with its binding activity, while GmFTL3 acted as a

174   regulator and GmFTL3/GmFDL complex directly inhibits *GmGRF5-1* expression.

175
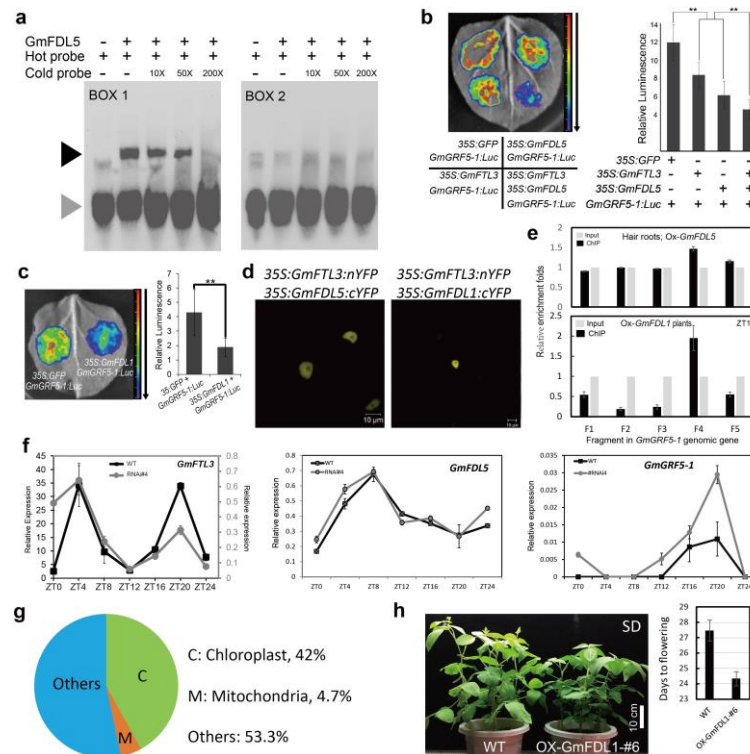
176 **Fig. 3 *GmFTL3*/*GmFDL* directly repress *GmGRF5-1* expression**. **a**, EMSA:

177 GmFDL5 bound to G-box 1 in *GmGRF5-1* promoter (Extended Data Fig. 5). **b**, **c**,

178 Luciferase bioluminescence assay: *GmGRF5-1:Luc* co-expressed with *35S:GmFTL3*

179 and *35S:GmFDL5* (**b**) or *35S:GmFDL1* (**c**). **d**, BiFC assay: GmFTL3 interacted with

180 GmFDL1/5. **e**, ChIP-qPCR: FDL5:GFP enriched special fragments (relative to input)

181 of *GmGRF5-1* promoter (Extended Data Fig. 5). **f**, RT-qPCR expression analysis of

182 *GmFTL3*, *GmFDL5* and *GmGRF5-1*. **g**, RNA-seq: Genes with over two-fold change

183 enriched to chloroplast (42%). **h**, Overexpressing *GmFDL1* soybean plants flowered

184 earlier. (n=12). Statistical analysis was done as Fig. 1.

185

186 ***GmGRF5-1* directly enhances vegetative growth**

187 To identify targets of *GmGRF5-1* controlling leaf growth and photosynthesis, we firstly carried

188 out transcriptome analysis of *GmFTL*-RNAi leaves and found that only a small fraction of

189 genes (0.378%, 212 out of 56,044 protein-coding loci) in the soybean genome (*Glycine max*

190 Wm82.a2.v1, https://phytozome.jgi.doe.gov/) showed more than twofold changes in gene

191 expression (Extend data Table 3), and RT-qPCR confirmed some of them (Extended Data

8

192   Fig. 3e). Among these, 42% of genes encoded proteins targeted to the chloroplast and 4.7%

193   of proteins targeted to the mitochondria (Fig. 3g), thereby suggesting that *GmFTL*-RNAi did

194   have a significant effect on energy metabolism in soybean.

195

196   In *Arabidopsis*, GRF regulates target gene expression through direct binding to a TGTCAGG

197   *cis*-element in target gene sequences[25]. We then randomly selected 10 genes from them as

198   potential *GmGRF5-1* target genes (*GTG*), due to their potential functions in photosynthesis

199   (Extend data Table 3) and their sequences containing at least one TGTCAGG *cis*-element

200   (Supplemental Information), a GRF binding sites[25]. These genes included hypothetical

201   chloroplast open reading frame (*YCF1, GTG1* here), NAD(P)H dehydrogenase subunit H

202   (*GTG2*), ATP synthase subunit alpha (*GTG3*), Plant basic secretory protein family protein

203   (*GTG4*), DNA-directed RNA polymerase family protein (*GTG5*), Photosystem II reaction

204   center protein D (*GTG6*), Photosynthetic electron transfer D (*GTG7*), Sucrose-proton

205   symporter 2 (*GTG8*), Phosphoenolpyruvate carboxylase-related kinase 2 (*GTG9*), Nucleotide-

206   sugar transporter family protein (*GTG10*). Surprisingly, *GmGRF5-1* significantly enhanced

207   expressions of most of *GTG* genes in tobacco cells (Fig. 4a, c, Extended Data Fig. 7a). Then,

208   we focused on *GTG1* gene, a member of *YCF* family with significant functions in gene

209   expression and photosynthesis[26]. In *35S:GmGRF5-1:MYC* transgenic soybean plants,

210   GmGRF5-1:MYC enriched Fragment 5 in the *GTG1* genome sequence (Fig. 4d, Extended

211   Data Fig. 5b). GmGRF5-1 proteins physically interacted with this fragment in an EMSA

212   analysis (Fig. 4e). What is more, in the presence of 35S-mini fragment, Fragment 4 and 5 of

213   *GTG1* could replace the full length of *GTG1* promoter and be activated by GmGRF5-1

214   proteins (Fig. 4b). In *GmGRF5-1:MYC* plants, not only there was an increase of *GTG1*

215   transcripts (Fig. 4f), but all of the leaf size, chlorophyll content, photosynthesis rate and

216   complexity of chloroplast increased (Fig. 4g, h, i), that contributed to plant yield (Fig. 5a).

217   Combining these results, we hypothesised that *GmFTL*-RNAi increased photosynthesis

218   through at least enhancing the expression of *GTG* genes mediated by *GmGRF5-1*.

219
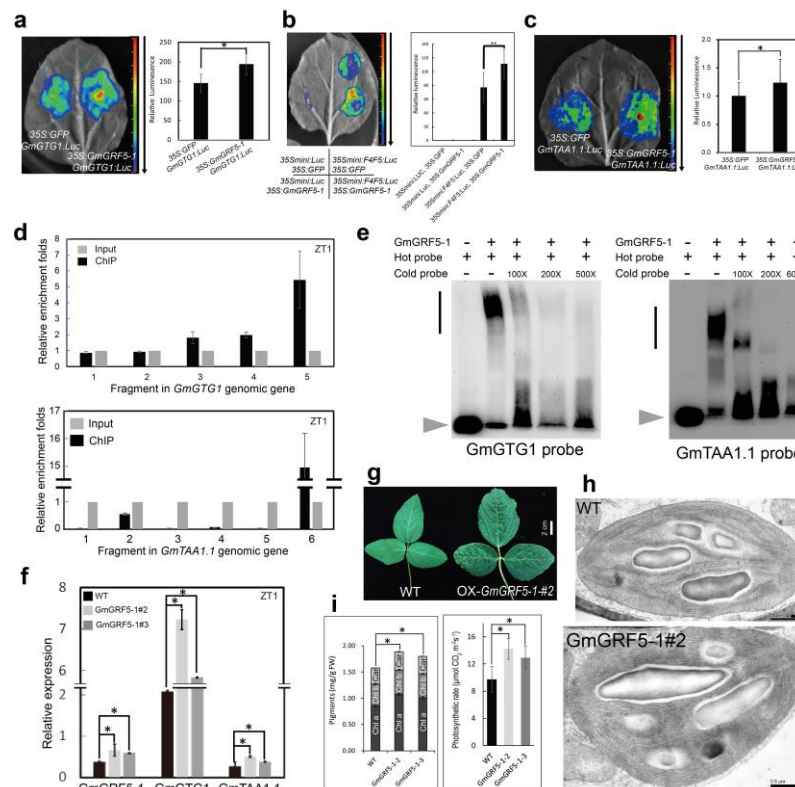
Fig. 4 *GmGRF5-1* directly enhances *GmGTG1* and *GmTAA1.1* expression. **a**, **b** and **c**, Luciferase bioluminescence assay: *GmGTG1:Luc* (**a**), *35Smini:F4F5:Luc* (*F4* and *F5* fragments of *GTG1* (**b**) or *GmTAA1.1:Luc* (**c**) were activated by *35S:GmGRF5-1*. **d**, ChIP-qPCR: GmGRF5-1:MYC enriched special fragments (relative to input) of *GmGTG1* or *GmTAA1.1* genes. **e**, EMSA: *GmGRF5-1* directly bound to special fragments of *GmGTG1* and *GmTAA1.1*. **f**, RT-qPCR assay of *GmGRF5-1*, *GmGTG1* and *GmTAA1.1* mRNA. **g**, The third trifoliolates. **h,** Chloroplasts in the third trifoliolates. Scale bar, 1 μm. **i,** The amounts of chlorophyll a, b and carotenoids and the net photosynthesis (n= 10 plants). The fragments tested (**b**, **d**, and **e**) are shown in Extended Data Fig. 5. Statistical analysis was done as Fig. 1.

As a result of larger organs and stature in *GmFTL*-RNAi and overexpressing-*GmGRF5-1* plants, we supposed auxin may be involved in such phenotypes because auxin is the main phytohormone controlling organ growth and development[27]. *TAA1* is a key gene gating auxin biosynthesis in many plants[28], and there are at least two *TAA1* homologs in the soybean genome (*GmTAA1.1-2*, Extended Data Fig. 7b). With similar strategy, we investigated the

237   effect of *GmGRF5-1* on *GmTAA1.1* gene. All results from luciferase luminescence assay (Fig.

238   4c), ChIP-qPCR (Fig. 4d), EMSA analysis (Fig. 4e), and gene expression (Fig. 4f) supported

239   that *GmGRF5-1* directly and positively regulated the expression of *GmTAA1.1* gene. And we

240   also proved that a GRF-binding *cis*-elements (Supplemental Information) in 3'UTR of

241   *GmTAA1.1* gene (Extended Data Fig. 5c) was a GmGRF5-1 targeting site. The results

242   indicated that *GmGRF5-1* may participate in auxin signalling pathway by directly and

243   positively regulating auxin biosynthesis.

244

245   **_GmGRF5-1_ directly represses _GmFTL3_ gene**

246   The overexpressing *GmGRF5-1* lines also displayed late flowering and higher yield per plant

247   (Fig. 5a), similar phenotypes of *GmFTL*-RNAi line (Fig. 1). By analysing the *GmFTL3* genomic

248   region, we found several potential GRF-binding *cis*-elements (Supplemental Information).

249   Therefore, we questioned whether *GmGRF5-1* could directly regulate *GmFTL* in a feedback

250   mode, and we exploited the similar approaches above to address it. The first line of evidence

251   from tobacco cells indicated that *GmGRF5-1* obviously inhibited expression of *GmFTL3*

252   genomic gene (Fig. 5b), but not *GmFDL5* (Fig. 5c). ChIP-qPCR isolated *GmGRF5-1:MYC*-

253   enriching Fragment 4 in *GmFTL3* genomic gene (Fig. 5e, Extended Data Fig. 5d), while

254   EMSA provided a strong line of evidence for direct binding of *GmGRF5-1* to this fragment

255   (Fig. 5d), which harboured a GRF *cis*-element (TGTCAGC) (Supplemental Information). Such

256   an inhibitory effect of *GmGRF5-1* on *GmFTL3* expression was confirmed by RT-qPCR for the

257   level of *GmFTL3* transcripts in the leaves of overexpressing *GmGRF5-1* lines (Fig. 5f). Thus,

258   a late-flowering phenotype of overexpressing *GmGRF5-1* plants may result from a direct and

259   negative effect of *GmGRF5-1* on *GmFTL3* expression.

260
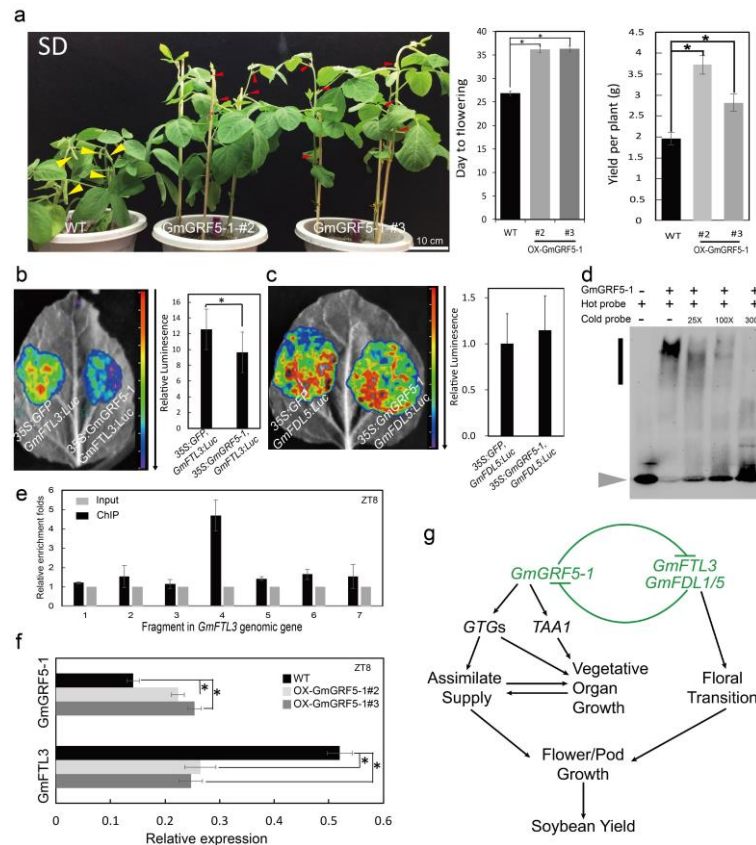
261 **Fig. 5 *GmGRF5-1* directly represses *GmFTL3* expression**. **a**, Overexpression

262 of *GmGRF5-1* delayed flowering and increased yield in soybean. Yellow arrows,

263 developing pods; red arrows, flowers. Scale bar, 10 cm. **b** and **c**, Luciferase

264 bioluminescence assay: *35S:GmGRF5-1* co-expressed with *GmFTL3:Luc* (**b**) or

265 *GmFDL5:Luc* (**c**). **d.** EMSA: GmGRF5-1 binds to Fragment 4 of *GmFTL3* gene

266 (Extended Data Fig. 5). **e**, ChIP-qPCR: GmGRF5-1:MYC enriched Fragment 4

267 (relative to input) in *GmFTL3* gene. **f**. RT-qPCR assay of *GmGRF5-1* and

268 *GmFTL3* mRNA. **g**. A repression feedback loop model showing the interaction of

269 *GmGRF5-1* and *GmFTL/GmFDL* balancing vegetative and reproductive growth.

270 Statistical analysis was done as Fig. 1.

271

272 **Discussion**

273 *FT* promotes flowering control[3,5,6], while *GRF5* enhances chloroplast growth, photosynthesis

274 and leaf growth[17]. Here, we identified a target gene of *FT* in leaves and a couple of target

275 genes of *GRF5* in soybean. Beyond flowering control, *FT* also plays vital roles in other

12

276   important processes, including the growth of tubers, bulbs and sugar beets, and seed

277   dormancy[9-11,13], even though leaf growth[6,14]. Regulation of *GmFTL* on *GmGRF5-1* enriches

278   our knowledge about florigen functions in leaf physiology. On the other hand, *GmGRF5-1*

279   feedback-represses *GmFTL3* expression. Based on our data, we propose a repression

280   feedback loop between *GmFTL*/*GmFDL* and *GmGRF5-1*, which plays a key role in balancing

281   vegetative growth and reproductive growth (Fig. 5g). *GmGRF5-1* enhances vegetative growth

282   through two pathways: one is related to metabolism through directly activating expression of

283   energy metabolism (photosynthesis) related genes including *YCF1* (*GTG1*, here)[26]; the other

284   is involved in organ growth through directly enhancing TAA1 expression (auxin synthesis[28]).

285   cytokinins is also associate with organ growth[17], while leaf growth may be aided by retrograde

286   signalling from the chloroplasts, as indicated in a previous study[29], a couple of energy-related

287   genes are positively regulated by *GmGRF5-1*. Positive interaction between the two pathways

288   increases assimilate supply for reproductive growth (flower and pod/seed growth). In contrast,

289   the *GmFTL*/*GmFDL* complex pushes plants going through floral transition and committing to

290   flowering and pod/seed development, which is supported by assimilate supply from vegetative

291   organs. Given that *GmGRF5-1* has no effect on *GmFDL* expression and that *GmFTL*

292   enhances *GmFDL* inhibitory effect on *GmGRF5-1*, *GmFDL* functions through its binding

293   activity to target DNA, as does *FD* in rice[23], and contributes to regulation of *GmFTL* on

294   *GmGRF5-1* expression. That means that the expression level of *GmFTL*, not *GmFDL*, mainly

295   determines the activity of the *GmFTL*/*GmFDL* complex in *GmGRF5-1* regulation in soybean.

296   The direction and intensity of plant development (vegetative or reproductive growth) are

297   manipulated by the repression-loop balance between *GmGRF5-1* and *GmFTL*/*GmFDL*.

298   Therefore, overexpressing-*GmGRF5-1* and *GmFTL*-RNAi soybean plants show similar

299   phenotypes, such as late flowering and high yield. Such a repression feedback loop is

300   commonly a regulatory motif for fine manipulation of various biological processes. For

301   example, the molecular circadian clock is maintained by repression feedback loops in

302   different organisms[30,31]. Because *FT* gene is a main integrator of multiple flowering

303   pathways[3,5,6], knocking-down of *GmFTL* expression affect only a small set of genes with

304   significant expression change (0.378%, here) and *FT* mutation results in very late flowering

305   and larger biomass[3,5,6], it is reasonable to believe that the repression-loop identified here may

306   play a key role in monitoring various environmental cues and buffering cell physiology to

307   adapt different stresses for plants to fulfil the life cycle.

308

309   Increased crop yield is required to feed a growing population[1], and researchers endeavour to

310   improve crop yields through studying different potential metabolic targets[32]. Our results

311   confirm that the repression feedback loop of *GmFTL*/*GmFDL* and *GmGRF5-1* can serve as a

312   new target to improve crop yield. For example, it is possible to fine-tune the expression of

313   *GmFTL* through RNAi approach to a level compatible to agricultural production to increase

314   crop yield in field. In this study, we improved soybean yield as much as 62% higher yield in

315   the field compared to wild type. *GmFTL*-RNAi line #3 may be a potential new elite of high

316   yield for soybean breeding in future. Several studies have indicated positive dosage effects of

317   the florigen gene *FT* on the yield of crops, including rice and tomato[7,8]. However, these

318   reports are based on genetic strategy (heterosis), which may not be easy to be transformed

319   into agricultural practice. It is credible to obtain much better elites with yield phenotype in the

320   field if constructing and screening more *GmFTL*-RNAi transgenic lines. What is more, any

321   cues controlling this repression feedback loop could be employed to modulate plant

322   development and translated into new targets of high yield. Due to high conservation of

323   *GmFTL*/*GmFDL* and *GmGRF5-1* genes across plants, the repression feedback loop may be

324   found in different plant species and the strategy of high yield here could be transferred to

325   other crops. To understand the function and regulation of the repression feedback loop in

326   spatial and temporal mode will help us to uncover plant development mechanism in more

327   detail and to exploit much more efficient strategy to increase crop yield.

328

329

330   **References:**

331   1   Tilman, D., Balzer, C., Hill, J. & Befort, B. L. Global food demand and the sustainable

332   intensification of agriculture. *Proc Natl Acad Sci U S A* **108**, 20260-20264,

333   doi:10.1073/pnas.1116437108 (2011).

334   2   Long, S. P., Marshall-Colon, A. & Zhu, X. G. Meeting the global food demand of the future by

335   engineering crop photosynthesis and yield potential. *Cell* **161**, 56-66,

336   doi:10.1016/j.cell.2015.03.019 (2015).

337   3   Blumel, M., Dally, N. & Jung, C. Flowering time regulation in crops-what did we learn from

338   Arabidopsis? *Curr Opin Biotechnol* **32**, 121-129, doi:10.1016/j.copbio.2014.11.023 (2015).

339   4   Hill, C. B. & Li, C. Genetic Architecture of Flowering Phenology in Cereals and Opportunities for

340   Crop Improvement. *Frontiers in plant science* **7**, 1906, doi:10.3389/fpls.2016.01906 (2016).

341   5   Andres, F. & Coupland, G. The genetic basis of flowering responses to seasonal cues. *Nat Rev*

342   *Genet* **13**, 627-639, doi:10.1038/nrg3291 (2012).

343   6   Yoo, S. K. *et al.* CONSTANS activates SUPPRESSOR OF OVEREXPRESSION OF CONSTANS 1 through

344   FLOWERING LOCUS T to promote flowering in Arabidopsis. *Plant Physiol* **139**, 770-778 (2005).

345   7   Krieger, U., Lippman, Z. B. & Zamir, D. The flowering gene SINGLE FLOWER TRUSS drives heterosis

346   for yield in tomato. *Nat Genet* **42**, 459-463, doi:10.1038/ng.550 (2010).

347   8   Huang, X. *et al.* Genomic architecture of heterosis for yield traits in rice. *Nature* **537**, 629-633,

348   doi:10.1038/nature19760 (2016).

349   9   Navarro, C. *et al.* Control of flowering and storage organ formation in potato by FLOWERING

350   LOCUS T. *Nature* **478**, 119-122, doi:10.1038/nature10431 (2011).

351 10 Lee, R., Baldwin, S., Kenel, F., McCallum, J. & Macknight, R. FLOWERING LOCUS T genes control

352   onion bulb formation and flowering. *Nature communications* **4**, 2884, doi:10.1038/ncomms3884

353   (2013).

354 11 Pin, P. A. *et al.* An antagonistic pair of FT homologs mediates the control of flowering time in

355   sugar beet. *Science* **330**, 1397-1400, doi:10.1126/science.1197004 (2010).

356 12 Hsu, C. Y. *et al.* FLOWERING LOCUS T duplication coordinates reproductive and vegetative growth

357   in perennial poplar. *Proc Natl Acad Sci U S A* **108**, 10756-10761, doi:10.1073/pnas.1104713108

358   (2011).

359 13 Chen, M. & Penfield, S. Feedback regulation of COOLAIR expression controls seed dormancy and

360   flowering time. *Science* **360**, 1014-1017, doi:10.1126/science.aar7361 (2018).

361   14   Teper-Bamnolker, P. & Samach, A. The flowering integrator FT regulates SEPALLATA3 and

362   FRUITFULL accumulation in Arabidopsis leaves. *The Plant cell* **17**, 2661-2675 (2005).

363   15   Omidbakhshfard, M. A., Proost, S., Fujikura, U. & Mueller-Roeber, B. Growth-Regulating Factors

364   (GRFs): A Small Transcription Factor Family with Important Functions in Plant Biology. *Molecular*

365   *plant* **8**, 998-1010, doi:10.1016/j.molp.2015.01.013 (2015).

366   16   Li, S. *et al.* Modulating plant growth-metabolism coordination for sustainable agriculture. *Nature*

367   **560**, 595-600, doi:10.1038/s41586-018-0415-5 (2018).

368   17   Vercruyssen, L. *et al.* GROWTH REGULATING FACTOR5 stimulates Arabidopsis chloroplast

369   division, photosynthesis, and leaf longevity. *Plant Physiol* **167**, 817-832,

370   doi:10.1104/pp.114.256180 (2015).

371   18   Guo, G. *et al.* Extensive Analysis of GmFTL and GmCOL Expression in Northern Soybean Cultivars

372   in Field Conditions. *PloS one* **10**, e0136601, doi:10.1371/journal.pone.0136601 (2015).

373   19   Kong, F. *et al.* Two coordinately regulated homologs of FLOWERING LOCUS T are involved in the

374   control of photoperiodic flowering in soybean. *Plant Physiol* **154**, 1220-1231,

375   doi:10.1104/pp.110.160796 (2010).

376   20   Fan, C. *et al.* Conserved CO-FT regulons contribute to the photoperiod flowering control in

377   soybean. *BMC Plant Biol* **14**, 9, doi:10.1186/1471-2229-14-9 (2014).

378   21   Contreras-Soto, R. I. *et al.* Genome-wide association mapping for flowering and maturity in

379   tropical soybean: implications for breeding strategies. *Breeding science* **67**, 435-449,

380   doi:10.1270/jsbbs.17024 (2017).

381   22   Ort, D. R. *et al.* Redesigning photosynthesis to sustainably meet global food and bioenergy

382   demand. *Proc Natl Acad Sci U S A* **112**, 8529-8536, doi:10.1073/pnas.1424031112 (2015).

383   23   Taoka, K. *et al.* 14-3-3 proteins act as intracellular receptors for rice Hd3a florigen. *Nature* **476**,

384   332-335, doi:nature10272 [pii]10.1038/nature10272 (2011).

385   24   Nan, H. *et al.* GmFT2a and GmFT5a redundantly and differentially regulate flowering through

386   interaction with and upregulation of the bZIP transcription factor GmFDL19 in soybean. *PloS one*

387   **9**, e97669, doi:10.1371/journal.pone.0097669 (2014).

16

388   25   Kim, J. S. *et al.* Arabidopsis growth-regulating factor7 functions as a transcriptional repressor of abscisic acid- and osmotic stress-responsive genes, including DREB2A. *The Plant cell* **24**, 3393-3405, doi:10.1105/tpc.112.100933 (2012).

391   26   Peter, E., Wallner, T., Wilde, A. & Grimm, B. Comparative functional analysis of two hypothetical chloroplast open reading frames (ycf) involved in chlorophyll biosynthesis from Synechocystis sp. PCC6803 and plants. *J Plant Physiol* **168**, 1380-1386, doi:10.1016/j.jplph.2011.01.014 (2011).

394   27   Leyser, O. Auxin Signaling. *Plant Physiol* **176**, 465-479, doi:10.1104/pp.17.00765 (2018).

395   28   Kasahara, H. Current aspects of auxin biosynthesis in plants. *Biosci Biotechnol Biochem* **80**, 34-42, doi:10.1080/09168451.2015.1086259 (2015).

397   29   Van Dingenen, J. *et al.* Chloroplasts Are Central Players in Sugar-Induced Leaf Growth. *Plant Physiol* **171**, 590-605, doi:10.1104/pp.15.01669 (2016).

399   30   Sato, T. K. *et al.* Feedback repression is required for mammalian circadian clock function. *Nature Genetics* **38**, 312-319, doi:10.1038/ng1745 (2006).

401   31   Huang, W. *et al.* Mapping the core of the Arabidopsis circadian clock defines the network structure of the oscillator. *Science* **336**, 75-79, doi:10.1126/science.1219075 (2012).

403   32   Ainsworth, E. A., Yendrek, C. R., Skoneczka, J. A. & Long, S. P. Accelerating yield potential in soybean: potential targets for biotechnological improvement. *Plant, cell & environment* **35**, 38-52, doi:10.1111/j.1365-3040.2011.02378.x (2012).

406

407

408   **Additional information**

409   **Extended Data Fig. 1** Agronomic traits of *GmFTL*-RNAi and wild type soybean plants

410   **Extended Data Fig. 2** Reduction of *GmFTL* mRNA promotes trifoliolate leaf growth

411   **Extended Data Fig. 3** Photosynthesis phenotype and transcriptome in *GmFTL*-RNAi line

412   **Extended Data Fig. 4** Alignment of GmGRF5-1 homologs and GmGRF5-1 protein subcellular localization

414   **Extended Data Fig. 5** Schematic representation of the genomic genes studied in this study

415   **Extended Data Fig. 6** GmFTL3 interacts in the nucleus with GmFDLs

bioRxiv preprint doi: https://doi.org/10.1101/437053; this version posted October 7, 2018. The copyright holder for this preprint (which was not certified by peer review) is the author/funder, who has granted bioRxiv a license to display the preprint in perpetuity. It is made available under aCC-BY-NC 4.0 International license.

421

431

432 **Author contributions**

433 Conceptualisation: Y.-F.F. and X.-M.Z.; Methodology: K.X., Y.-F.F., G.Y., X.-M.Z., M.L., C.L.

434 and H.C.; Investigation: K.X., X.-M.Z., G.Y., M.L., C.L., H.C., Y.-F.F., J. Z., F.C., Z.C., P.H,

435 Y.M. and L.L.; Formal analysis and validation: K.X., X.-M.Z., G.Y., I.S., M.L. and Y.-F.F.;

436 Visualisation: K.X. and Y.-F.F.; Writing—original draft: Y.-F.F. and K.X.; Writing—review and

437 editing: I.S. and Y.-F.F.; Funding acquisition: X.F., X.-M.Z. and Y.-F.F.; Project administration:

438 Y.-F.F. and X.-M.Z.; Resources: X.Z, Y.-F.F., Y.M., Q.C and I.S.; Supervision: Y.-F.F.

439

440 **Author information**

441 Kun Xu[1*], Xiao-Mei Zhang[1*], Guolong Yu[2*], Mingyang Lu[1*], Chunyan Liu[2*], Haifeng Chen[3*],

442 Jinlong Zhu[1], Fulu Chen[1], Zhiyuan Cheng[1], Penghui Huang[1], Xinan Zhou[3], Qingshan Chen[2],

443 Xianzhong Feng[4], Yuchen Miao[5], Liangyu Liu[6], Iain Searle[7], Yong-Fu Fu[1§]

444

445 [1] MOA Key Laboratory of Soybean Biology (Beijing), National Key Facility of Crop Gene

446 Resource and Genetic Improvement, Institute of Crop Sciences, Chinese Academy of

447 Agricultural Sciences, Nandajie 12, Zhongguancun, Haidian District, 100081 Beijing, China

448 [2] Key Laboratory of Soybean Biology, Ministry of Education/College of Agriculture, Northeast

449 Agricultural University, Harbin 150030, China

450 [3] Oil Crops Research Institute, Chinese Academy of Agricultural Sciences, Key Laboratory of

451 Biology and Genetic Improvement of Oil Crops, Ministry of Agriculture, Wuhan, 430062,

452 China

453 [4] CAS Key Laboratory of Soybean Molecular Design Breeding, Northeast Institute of

454 Geography and Agroecology, Chinese Academy of Sciences, Changchun 130102, China

455 [5] Key Laboratory of Plant Stress Biology, State Key Laboratory of Cotton Biology, School of

456 Life Sciences, Henan University, Kaifeng 475004, China

457 [6] College of Life Sciences, Capital Normal University, Beijing 100048, China

458 [7] School of Biological Sciences, School of Agriculture, Food and Wine, The University of

459 Adelaide, Adelaide, 5005, Australia.

460

461 [*] These authors contributed equally.

462

463 [§] To whom correspondence should be addressed to fuyongfu@caas.cn or

464 fufu19cn@163.com. Telephone/Fax: +86-10-82105864

465 **Declaration of interest:** The authors declare no competing interests.

466

467 **METHODS**

468 **Plant materials and growth conditions**

469 *GmFTL*-RNAi plants were previously generated in the soybean (*Glycine max* (L.) Mer.)

470 cultivar Tianlong1 in our lab[18]. All RNAi lines used here are independent, homozygous,

471 transgenic lines. Wild type soybean controls for all experiments was cultivar Tianlong1. All

472   plants were grown in controlled temperature and photoperiod growth rooms, greenhouses

473   and/or the field. The light conditions in the plant growth rooms were short day conditions (8 hr

474   light / 16 hr dark) from a LED light source with intensities ranging from 500 µmol·m^{-1}·s^{-1} at soil

475   level to 800 µmol·m^{-1}·s^{-1} at the top of plants at maturity. Soybean field (plot) experiments were

476   carried out at Hanchun (N30°22', E113°22') and Beijing (N39°58', E116°20'). Spring sown

477   soybeans were planted on 23rd April 2016 for Hanchun, and 15th May 15 or 1st June 2017 for

478   Beijing. The plot area was 300 × 225 cm^2 with 45 cm of row-spacing and 20 cm of plant-

479   spacing at Hanchun or 600 X 300 cm^2 with 60 cm of row-spacing and 30 cm of plant-spacing

480   at Beijing. Agronomic characters were observed at maturity. Individual plants from each plot

481   were subjected to statistical analysis.

482

483   **Plasmid construction and plant transformation**

484   The encoding full-length sequence of *GmGRF5-1* was cloned into the binary vector

485   pFGC5941-GW, a modified vector from pFGC5941, by an LR reaction to generate binary

486   vector *35S*:*GmGRF5-1*:*MYC*, which was introduced into soybean cultivar Tianlong1 through

487   cotyledon node transformation mediated by *Agrobacterium tumefaciens*. Transgenic lines

488   were selected by Basta® herbicidie resistance and transgene expression was measured by

489   RT-qPCR.

490

491   To express His-tagged proteins in *E. coli*, *GmFDL5* and *GmGRF5-1* genes were cloned into

492   pET28a (Novagen) with *Xba* I/*Bam*H I or *Nde* I/*Xho* I restriction enzyme sites, respectively.

493   For *GmGRF5-1* promoter activity and ChIP analysis, the coding sequences of *GmFTL3*,

494   *GmFDL5* and *GmFDL1* and the promoter sequence of *GmGRF5-1* were cloned into pGWC[33],

495   respectively. Then, pGWC-*GmFTL3*, pGWC-*GmFDL5* and pGWC-*GmFDL1* genes were LR-

496   reacted with pGWB5 by LR reactions (Invitrogen) to get binary vectors of pGWB5-*GmFTL3*,

497   pGWB5-*GmFDL5* and pGWB5-*GmFDL1*. pGWC-*GmGRF5-1* was combined with pGWB35 by

498   LR reactions (Invitrogen) to get plant expressing vector of pGWB35-*GmGRF5-1*. For

499   GmFDL5 and GmFDL1 ChIP experiment, the pGWB5-*GmFDL5* was used to root hair

500   transformation, while pGWB5-*GmFDL1* vectors was employed for soybean stable

501   transformation.

502

503   For other promoter analyses, the promoter and fragment sequences of interest were cloned

504   into entry clone Fu76 (this lab) recombined into pSoy2 (this lab) by LR reactions (Invitrogen)

505   to generate pSoy2-Luc destination clones[34]. pGWB6 was used to express GFP as a negative

506   control. The promoter and fragment sequences were listed in Supplemental Information.

507

508   For BiFC assays, *GmFTL3*, *GmFDL5* and *GmFDL1*genes were cloned into pGWC. Then, by

509   LR reactions (Invitrogen), the full length *GmFTL3* gene was cloned into pEarlyGate201 to

510   generate a *GmFTL3-nYFP* binary vector, while full length *GmFDL5* and *GmFDL1* genes were

511   cloned into pEarlyGate202 recombined to create *GmFDL5-cYFP* or *GmFDL1-cYFP* binary

512   vectors.

513

514   *GmGRF5-1* gene was cloned into Fu28[34] and the subsequent GFP-tagged gene pSoy2-

515   *GmGRF5-1* was used for cellular localization analysis.

516

517   All PCR amplified genes used in this study were confirmed by Sanger sequencing. The

518   sequences of the genes and promoters are listed in Supplemental Information. The

519   description of genes and primer sequences for genes are listed in Extend data Table 1 and 2,

520   respectively.

521

522   **RNA extraction and expression analysis**

523   For RT-qPCR analysis, total RNA was extracted using EasyPure® RNA Kit (ER101-01,

524   TransGen Biotech). The quantity was measured by Nanodrop 2000C (ThermoFisher

525   Scientific). For SYBR detection of RT-qPCR products, 500-1000 ng of the total RNA was used

526   for reverse transcription (KR106-02, TIANGEN). SYBR Premix Ex-Taq (Perfect Real Time;

527   TAKaRa) was used for the RT-qPCR assays. For TaqMan analysis, about 1 μg of total RNA

528   was used for reverse transcription (KR106-02, TIANGEN), TaqMan™ Gene Expression

529   Master Mix (No.4369016, ThermoFisher Scientific) was used for the RT-qPCR assays. The

530   RT-qPCR was conducted using StepOne Plus (ABI). The reference genes *GmACT11* or

531   *GmUKN2* were used as internal controls for normalization of all SYBR RT-qPCR data.

532   Sequences of the primers are listed in Extend data Table 2. The $2^{-\Delta CT}$ method was used to

533   calculate the relative expression levels based on three technical replicates.

534

535   **Electrophoretic mobility shift assay (EMSA)**

536   Recombinant proteins were purified from *E. coli* BL21 cells using nickel beads (No.31014,

537   QIAGEN) for His-GmFDL5 or His-magnetic beads (Beaver Company, China) for His-

538   GmGRF5-1 and purity confirmed by western blotting using an anti-His antibody (AbMart

539   company, China). The purified proteins were dialyzed against Tris-HCl buffers (25 mM, pH

540   7.5) to remove contaminating imidazole. Biotin was used to label the 5' end of both sense and

541   antisense oligo probes. Probes were heated and cooled to obtain probe duplexes. The biotin-

542   labeled DNA was synthesized by Invitrogen (Shanghai, China) for *GmGRF5-1* and BGI

543   (China) for *GmFTL3* and *GmGTG1*, respectively. EMSA was carried out according to the

544   manufacturer's protocol for Light Shift Chemiluminescent EMSA kit (No. 20148, ThermoFisher

545   Scientific). The binding buffer for *GmFDL5* protein binding assays contained 10 mM Tris-HCl

546   (pH 7.5), 50 mM KCl, 1 mM DTT, 2.5% glycerol, 5 mM $MgCl_2$, 50 g·µl^{-1} poly(dI·dC), 0.05%

547   NP-40, while the binding buffer for GmGRF5-1 protein binding assay consisted of 10 mM Tris-

548   HCl (pH 8.7), 50 mM KCl, 5 mM $MgCl_2$, 10 mM DTT, 2.5% glycerol, 20 mM EDTA. Each 20 µl

549   binding reaction contained 1 fmol of biotin-labeled, unlabeled dsDNA at different

550   concentrations and recombinant His-tag proteins. Binding reactions were incubated for 30 min

551   at 22°C. The reactions were separated on a 5% polyacrylamide gel for GmFDL5/GmGRF5-1

552   complex, or an 8% precast SurePage™ Gel (GenScript, China) for GmGRF5-1/GmFTL3.F4,

553   GmGRF5-1/GmGTG1.F5 and GmGRF5-1/GmTAA1.1F6 complex binding assays. The

554   running buffer used was TBE (pH 8.0) for GmFTL5 proteins or TBE (pH 8.75) for GmGRF5-1

555   proteins. Detection of biotin-labeled DNA was performed by chemiluminescence using a

556   ChemiDoc-It Imaging System (UVP, Cambridge, UK).

557

Bimolecular fluorescence complementation (BiFC)

559   The pEarlyGate201-*GmFTL3-nYFP* and pEarlyGate202-*GmFDL5-cYFP* or pEarlyGate202-

560   *GmFDL1-cYFP* binary vectors were transiently expressed using *Agrobacterium tumefaciens*.

561   Both recombinant *Agrobacterium* cells were co-infiltrated into *Nicotiana benthamiana* leaves.

562   Empty vectors were used as negative controls and AtAHL22-RFP was used as a nuclear

563   marker. *N. benthamiana* was grown under long-day (16 hr light:8 hr dark) conditions at 22℃

564   for at least 48 hours post infiltration. Leaves were observed under a confocal microscope

565   (Zeiss LSM700).

566

Luciferase bioluminescence assays

568   Luciferase assays were performed as previously outlined with some minor modifications[35].

569   Briefly, *A. tumefaciens* containing different vectors were co-infiltrated into 4-week-old *N.*

570   *benthamiana* leaves. After co-infiltration, the plants were then grown in darkness for 12 hours

571   and subsequently grown under long-day conditions (16hr Light:8hr Dark) for 1 day. Prior to

572   bioluminescence imaging, co-infiltrated leaves were uniformly sprayed with 2 mM D-luciferin

573   (Gold Biotechnology) diluted in 0.01% Triton X-100 solution. After spraying with D-luciferin,

574   leaf samples were incubated in the dark for 5 min. Exposure times for luminescence imaging

575   were 3-5 min. Imaging of bioluminescence signals were performed using a NightShade LB

576   985 *In vivo* Plant Imaging System (Berthold Technologies, Germany). IndiGO Imaging

577   Software (Berthold Technologies, Germany) was used for image acquisition and processing

578   of luminescence. At least ten leaves for each experiment were used, and each experiment

579   was repeated at least three times. All potential promoter sequences of genes except *GmFTL3*

580   and *GmTAA1.1* were employed in this study. The full sequence of promoter, 5'UTR, genomic

581   gene and 3'UTR of *GmFTL3* (Figure 5D) was used for this assay and the luciferase gene was

582   inserted just before the stop codon of *GmFTL3* gene. The sequence of promoter and 3'UTR

583   of *GmTAA1.1* was used to analyze *GmGRF5-1* activity on Gm*TAA1.1* regulation. All promoter

23

584   sequences fused to luciferase are listed in Supplemental Information.

585

Chromatin immunoprecipitation (ChIP) qPCR analyses

587   Chromatin was extracted from leaves or roots of soybean plants grown under short day

588   conditions. Tissue was harvested at zeitgeber 1 (ZT1) timepoint. ChIP-qPCR assays were

589   performed essentially as described[36] with minor modifications: (1) cross-linking duration was

590   30 min with three intervals for stirring the solution to remove bubbles on the surface of leaves,

591   (2) sonication time was 20 min, (3) two steps were employed to reverse cross-link, that

592   included NaCl (300 mM) incubation overnight at 65°C and 1% Chelex-100 for 15 min at 95°C.

593   The sonicated DNA were used for immunoprecipitation with commercially available anti-GFP-

594   mAb-magnetic beads (MBL, D153-11) for the GmFDL5-GFP assay and anti-Myc-mAb-

595   magnetic agarose (MBL, Mo47-10) for GmGRF5-1 assay. After reversing the cross-linking,

596   immunoprecipitated DNA was analyzed by qPCR using primers (Supplemental Table S1) for

597   specific regions. For the GmGRF5-1 binding assay, the regions for qPCR analysis contained

598   at least one of the AtGRF7 protein binding motifs (TGTCAGG[25]) or its derivatives (TGTCAAG,

599   TGTGAAG, TGTTAGG, TTTCAGG, GATCAGG, GTTCAGG, TGTCATG, TGGCAGG,

600   CTTCAGG, TGTCACG TGTTATG). Three independent experiments, each using around 1 g

601   of leaves were performed. Three technical replicates for each qPCR were carried out and

602   Gm*ACT11* or *GmUKN2* were used as internal controls for normalization. Each experiment

603   was repeated at least three times.

604

Chloroplast analysis and chlorophyll measurements

606   The fully-opened third and seventh trifoliolate leaves of soil-grown greenhouse WT (cv.

607   Tianlong1) and *GmFTL*-RNAi line 4 soybean plants were harvested for the measurements.

608   Perpendicular transverse sections of the middle leaflets of trifoliolate leaves were prepared by

609   the Transmission-Electron-Microscope and Mass-Spectrometry Platform of Institute of

610   agricultural products processing, Chinese Academy of Agricultural Sciences (Beijing, China).

611   The photos were obtained by using a transmission electron microscope (H-7500, Japan).

24

612 Microscopic differential interference contrast images were taken, the area of 200 mesophyll

613 cells flanking the epidermis was measured by using ImageJ software. Chloroplast number per

614 leaf area and chloroplast number per cell were measured by using Image J software.

615

616 For chlorophyll content analysis, we punched 20 fresh sections (d = 6 mm) from five individual

617 leaves for each sample by using a hole puncher. The samples were immersed in 25 mL of

618 80% acetone, and stored at room temperature for 5 days. Then 1 mL of the supernatants was

619 measured for absorbance at 663 and 645 nm. The concentration of chlorophyll a and b (Chl a

620 and Chl b) and carotenoids was calculated using the following formulas:

621

622 $$Chl\ a = (11.24A_{662} - 2.04A_{645}) \times V / W$$

623 $$Chl\ b = (20.13A_{645} - 4.19A_{662}) \times V / W$$

624 $$Carotenoids = ((1000A_{470} - 1.90\ Chl\ a - 63.14\ Chl\ b) / 214) \times V / W$$

625 (V for the volume of acetone, W for the fresh weight of the sample)

626

627 **Photosynthetic rate and chlorophyll fluorescence analyses**

628 Plants were grown under SD conditions, and the third trifoliolate leaves (n = 10) of WT (cv.

629 Tianlong1) and *GmFTL*-RNAi line 4 line were selected for measuring the photosynthetic rates

630 at days 28 to 35 after sowing following the manufacturer's instructions (LICOR LI-6400

631 V4.0.1). Fv/Fm was measured using an IMAGING-PAM M series Chlorophyll Fluorometer

632 with the MAXI version (Heinz Walz, Effeltrich, Germany). SD grown plants were placed in

633 darkness for 30 min before measurements were taken.

634

635 **Measurement of sugar content in leaves**

636 WT (cv. Tianlong1) and *GmFTL*-RNAi line 4 seeds were sown in spring 2015 and grown at

637 Beijing (China). Third fully-opened trifoliolate leaves were harvested at one hour after sunset

638 for the measurement of sugar contents (n = 5). For the extraction of soluble sugars and

639 starch, about 100 mg of leaf samples were homogenized in 0.5 mL of 80% (v/v) ethanol in a

25

640   1.5-mL tube and incubated at 70°C for 90 min. Following centrifugation at 16,000 g for 5 min,

641   the supernatant was transferred to a new 1.5 mL tube. The pellet was rinsed twice with 2 mL

642   of 80% ethanol and removed. Any remaining solvent was evaporated at room temperature by

643   using a vacuum. The residue was resuspended in 0.3 mL of distilled, sterile water and this

644   represented the soluble carbohydrate fraction. The remaining pellet contained the insoluble

645   carbohydrates, included starch, was homogenized in 0.2 mL of 0.2 N KOH and the

646   suspension was incubated at 95°C for 1 hr to dissolve the starch. Following the addition of

647   0.035 mL of 1 N acetic acid and centrifugation for 5 min at 16,000 g, the supernatant was

648   used for starch quantification. Detailed procedures were followed according to the

649   manufacturer's instructions; starch (No. 1013910603), Maltose/Sucrose/D-Glucose (No.

650   11113950035) and D-Glucose/D-Fructose kits (No. 10139106035) (R-Biopharm, Germany).

651

652   **Measurement of leaflet area**

653   When the trifoliolates were fully opened (plants were grown in greenhouse), the length and

654   width of each leaflet were measured. And so on, for each of trifoliolates of indicated lines.

655   Leaflet area was calculated using the formula d = (L + 2W) / 3 (d indicates the diameter; L

656   represents the length of leaflet; W represents the width of leaflet). (n = 7 plants)

657

658   **Leaf anatomical structure analysis**

659   Fully-opened third or seventh trifoliolate leaves of soil-grown, glasshouse plants of WT or

660   *GmFTL*-RNAi line 4 plants were excised. The leaves were fixed in FAA fixative solution

661   (formaldehyde solution 5 ml: glacial acetic acid 5 ml: 70% ethanol 90 mL). Perpendicular

662   transverse sections were prepared through the middle leaflets of trifoliolate leaves by

663   Servicebio Biotechnology Co Ltd (Wuhan, China). The sections were observed, and

664   photographs were obtained by using a SteREO Discovery V20 (Zeiss, Germany).

665

666   **Measurement of major agronomic traits**

667   The flowering time was determined by emergence of the first flower on the main stem of

668   soybean plants. Podding time was determined as the time when the first pod on the main

669   stem was 2 cm in length. Measurements of plant height, branch number, node number, pod

670   number and seed number per plant were performed at full plant maturity. For experiments in

671   both the greenhouse and growth rooms, more than ten individual plants of each line were

672   sampled for analysis of all those traits. To examine field yield traits, three plot replications

673   were used at Beijing (N39°58', E116°20') and Hanchuan (N30°63', E113°591) sites for each

674   indicated line. For the Beijing field experimental site, the planting density was 30 cm × 60 cm,

675   with one plant per site. The area per plot was 14.4 m^2. For the Hanchuan plot site, the

676   planting density was 20 cm × 50 cm, with two plants per site. The area per plot was 6 m^2.

677

678   **Measurement of leaflet area**

679   When the first trifoliolate leaves were fully opened, the length and width of each leaflet of

680   plants (n = 7 plants) grown in the greenhouse were measured. Leaflet area was calculated

681   using the formula d = (L + 2W) / 3 (where d indicates the diameter; L represents the length of

682   the leaflet; W represents the width of the leaflet).

683

684   **Transcriptome analysis**

685   The fully-opened third trifoliolate leaves from WT or *GmFTL*-RNAi line 4 line plants were

686   sampled one hour after sunrise. Total RNA was extracted using EasyPure® RNA Kit (ER101-

687   01, TransGen Biotech). RNA sequencing by an Illumina HiSeq instrument and data analysis

688   were performed by Biomarker Technologies (Beijing, China). Illumina sequencing reads were

689   mapped to reference genome *Glycine max* Wm82.a2.v1

690   (https://phytozome.jgi.doe.gov/pz/portal.htm).

691

692   **Statistical analysis**

693   All experiments in this study were carried out at least three times, all of which showed similar

694   results. The figures show only a representative result. Data in all bar graphs represent the

695   mean ± SD. For digital statistical analysis, all statistical analyses were determined using

27

696 SPSS software package. Asterisks indicate significant difference according to a Student's *t*-

697 test (**$P < 0.01$, * $P < 0.05$).

698

699 **Accession Numbers**

700 Sequence data from this article can be found in Supplemental Information, and their

701 corresponding identities are listed in Extended Data Table 1.

702

703 **References:**

704 33. Chen, Q. J., Zhou, H. M., Chen, J. & Wang, X. C. Using a modified TA cloning method to create

705 entry clones. *Anal Biochem* **358**, 120-125 (2006).

706 34. Wang, X., Fan, C., Zhang, X., Zhu, J. & Fu, Y. F. BioVector, a flexible system for gene specific-

707 expression in plants. *BMC Plant Biol* **13**, 198, doi:10.1186/1471-2229-13-198 (2013).

708 35. Song, S. *et al.* The Jasmonate-ZIM Domain Proteins Interact with the R2R3-MYB Transcription

709 Factors MYB21 and MYB24 to Affect Jasmonate-Regulated Stamen Development in Arabidopsis.

710 *Plant Cell* **23**, 1000-1013 (2011).

711 36. Saleh, A., Alvarez-Venegas, R. & Avramova, Z. An efficient chromatin immunoprecipitation (ChIP)

712 protocol for studying histone modifications in Arabidopsis plants. *Nature protocols* **3**, 1018-1025,

713 doi:10.1038/nprot.2008.66 (2008).

714

715